American Mineralogist, Volume 94, pages 609–615, 2009

Fettelite, $[Ag_6As_2S_7][Ag_{10}HgAs_2S_8]$ from Chañarcillo, Chile: Crystal structure, pseudosymmetry, twinning, and revised chemical formula

Luca Bindi,[1,*] Frank N. Keutsch,[2] Carl A. Francis,[3] and Silvio Menchetti[4]

[1]Museo di Storia Naturale, Sezione di Mineralogia, Università di Firenze, Via La Pira 4, I-50121 Firenze, Italy
[2]Department of Chemistry, University of Wisconsin-Madison, 1101 University Avenue, Madison, Wisconsin 53706, U.S.A.
[3]Harvard Mineralogical Museum, Harvard University, 24 Oxford Street, Cambridge, Massachusetts 02138, U.S.A.
[4]Dipartimento di Scienze della Terra, Università di Firenze, Via La Pira 4, I-50121 Firenze, Italy

Abstract

The crystal structure of the rare mineral fettelite was solved using intensity data collected from a twinned crystal from Chañarcillo, Copiapó Province, Chile. This study revealed that, in spite of the strong hexagonal pseudosymmetry, the structure is monoclinic (space group *C*2) with $a = 26.0388(10)$, $b = 15.0651(8)$, $c = 15.5361(8)$ Å, $\beta = 90.48(1)°$, and $V = 6094.2(5)$ Å^3. The refinement of an anisotropic model led to an *R* index of 0.0656 for 7143 observed reflections [$I > 2\sigma(I)$] and 0.0759 for all 17 447 independent reflections. Fettelite is intimately twinned with six twin domains. The structure consists of the stacking of two module layers along [001]: an *A* module layer with composition $[Ag_6As_2S_7]^{2-}$ and a *B* module layer with composition $[Ag_{10}HgAs_2S_8]^{2+}$. The As atoms form isolated AsS_3 pyramids typical of sulfosalts, Hg links two sulfur atoms in linear coordination, and Ag occupies sites with coordination ranging from quasi linear to almost tetrahedral. The *A* module layer found for fettelite is identical to that described for the minerals belonging to the pearceite-polybasite group. On the basis of information gained from this characterization the crystal chemical formula was revised according to the structural results, yielding $[Ag_6As_2S_7][Ag_{10}HgAs_2S_8]$ ($Z = 8$).

Keywords: Silver sulfosalts, crystal structure, chemical composition, optical properties, fettelite, pearceite-polybasite, polytypes, physical properties

Introduction

Fettelite, ideally $Ag_{24}HgAs_5S_{20}$, was identified as an independent mineral species by Wang and Paniagua (1996) during a study of silver sulfosalts from the Glasberg quarry, Nieder-Beerbach, Odenwald, southwestern Germany, and was named in honor of M. Fettel, a field geologist who is well recognized for his work in the area. By means of precession photographs and powder X-ray investigation these authors gave a hexagonal unit cell for fettelite, $a = 15.00$, $c = 15.46$ Å, and reported that the mineral could crystallize in one of the following possible space groups: *P*312, *P*321, *P*31*m*, *P*3*m*1, *P*$\bar{3}$1*m*, or *P*$\bar{3}$*m*1. However, Wang and Paniagua (1996) were not able to proceed to a crystal-structure determination of fettelite at that time. More recently, Pérez-Priede et al. (2005) investigated the crystal structure of fettelite and reported that fettelite exhibits hexagonal rings of metal and sulfur atoms that are linked by sharing their edges, giving rise to parallel sheets when viewed along the **c** axis. The sheets are joined creating a three dimensional network (Pérez-Priede et al. 2005). Nevertheless, a full paper describing the details of the crystal structure is yet to appear in the scientific literature.

In the course of a study dealing with the characterization of structurally complex silver-bearing minerals of mineralogical collections from various museums (Bindi et al. 2007a and references therein), fettelite was obtained from another occurrence. In this paper, we report the crystal structure of fettelite together with physical and chemical data for this mineral.

Occurrence

The sample containing the fettelite crystal used in the present study (Harvard Mineralogical Museum cat. number 140586) is from Chañarcillo, Copiapó Province, Chile, a nineteenth century silver mining district famous for its supergene and oxidized ores from veins cutting Cretaceous limestones. The geology and mineralogy of Chañarcillo are reviewed by Cook (1979). As the distinguishing chemical feature of fettelite is its mercury content, it is interesting that Cook remarks "Perhaps the most unusual mineral occurring at Chañarcillo is moschellandsbergite. This compound of silver and mercury occurs in silver-white metallic cubes of rather small size. The presence of this and other mercury-bearing secondary minerals at Chañarcillo has not been adequately explained with respect to the mineralogy of the primary veins that in all likelihood were the ultimate source of the mercury." A moschellandsbergite specimen in the F. Keutsch collection has cinnabar associated establishing the identity of the primary mercury mineral at Chañarcillo.

Fettelite was discovered when a large specimen of crystallized proustite was subdivided. Fettelite occurs in two associations on crystals of proustite where it is abundant as thin dark red metallic plates (up to 1 cm in size) in subparallel to radiating

* E-mail: luca.bindi@unifi.it

crystals spanning small vugs in the calcite-proustite matrix. It also occurs as ruby-colored, mica-like flakes up to 0.1 cm in size dispersed on palygorskite overlying the druse of centimeter-sized scalenohedral proustite crystals. It is the fettelite from the latter material that was selected here for study.

This contribution establishes Chañarcillo as the second known occurrence of fettelite. At Chañarcillo, fettelite was an unrecognized minor ore mineral occurring with proustite, on the order of several grams in weight, whereas fettelite at the Glasberg quarry is a rare species observed only under the microscope. Our discovery of fettelite on museum specimens from Chañarcillo suggests that additional fettelite specimens will be recognized in the future.

Like most specimens from Chañarcillo that are preserved in museum collections, the specific mine from which sample 140586 was collected is not recorded. Although the Dolores mine is frequently cited as the source of the finest Chañarcillo proustite specimens, there is no information to show that sample 140586 comes from the Dolores mine, one of more than one hundred mines in the Chañarcillo area.

Chemical composition

A preliminary chemical analysis using energy dispersive spectrometry, performed on the crystal fragment used for the structural study, did not indicate the presence of elements ($Z > 9$) other than S, As, Ag, Sb, and Hg, with very minor Fe, Cu, Tl, and Pb. The chemical composition was then determined using wavelength dispersive analysis (WDS) by means of a JEOL JXA-8600 electron microprobe. Major and minor elements were determined at an accelerating voltage of 20 kV and a beam current of 40 nA, with 10 s as counting time. For the WDS analyses the following lines were used: S$K\alpha$, Fe$K\alpha$, Cu$K\alpha$, Zn$K\alpha$, As$L\alpha$, Se$L\alpha$, Ag$L\alpha$, Sb$L\beta$, Te$L\alpha$, Hg$L\alpha$, Tl$M\alpha$, and Pb$M\alpha$. The standards employed were: pure metals for Cu, Ag, Tl, and Te; galena for Pb; pyrite for Fe and S; cinnabar for Hg; synthetic Sb_2S_3 for Sb; synthetic As_2S_3 for As; synthetic ZnS for Zn; and synthetic $PtSe_2$ for Se. The fettelite fragment was found to be homogeneous within analytical error. The average chemical composition (eight analyses on different spots), the ranges of wt% of elements, and the atomic ratios on the basis of 36 and 50 atoms for the fettelite crystal studied here are reported in Table 1, together with the chemical data given by Wang and Paniagua (1996) for the type fettelite. On the basis of 36 atoms (see hereafter the structure description), the formula of the fettelite crystal from Chile can be written as $(Ag_{15.92}Cu_{0.04}Pb_{0.02}Fe_{0.01}Tl_{0.01})_{\Sigma=16.00}Hg_{0.98}(As_{3.65}Sb_{0.35})_{\Sigma=4.00}S_{15.02}$.

Table 1. Electron microprobe data (means and ranges in wt% of elements) and atomic ratios (on the basis of 36 and 50 atoms, respectively) for fettelite

	Mean and ranges (wt% el.)	Atomic ratios ($\Sigma_{atoms} = 36$)	Atomic ratios ($\Sigma_{atoms} = 50$)
Fettelite from Chañarcillo, Chile (this study)			
Ag	62.78 (62.22–63.09)	15.92	22.11
Cu	0.09 (0.04–0.12)	0.04	0.05
Pb	0.15 (0.07–0.18)	0.02	0.03
Tl	0.07 (0.05–0.15)	0.01	0.01
Fe	0.02 (0.00–0.03)	0.01	0.01
Hg	7.19 (7.00–7.36)	0.98	1.36
As	10.01 (9.55–10.27)	3.65	5.08
Sb	1.56 (1.40–1.66)	0.35	0.49
S	17.60 (17.29–17.77)	15.02	20.86
Total	99.47 (99.15–100.13)	36.00	50.00
Fettelite from the type locality (Wang and Paniagua 1996)			
Ag	67.55 (67.45–68.84)	17.19	23.88
Cu	0.07 (0.06–0.08)	0.03	0.04
Pb	0.07 (0.02–0.16)	0.01	0.01
Tl	0.13 (0.06–0.23)	0.02	0.02
Fe	0.04 (0.03–0.04)	0.02	0.03
Hg	5.21 (5.12–5.38)	0.71	0.99
As	9.80 (9.19–10.33)	3.59	4.99
Sb	0.23 (0.17–0.36)	0.05	0.07
S	16.79 (16.18–17.01)	14.38	19.97
Total	99.89 (99.60–100.61)	36.00	50.00

Physical and optical properties

Fettelite from Chañarcillo is dark violet to red in color and shows a dark vermillion streak. The mineral is opaque in transmitted light and exhibits a metallic luster. The crystals are brittle with perfect {001} cleavage and the fracture is uneven to subconchoidal. Micro-indentation measurements carried out with a VHN load of 20 g give a mean value of 139 kg/mm^2 (range: 125–144), corresponding to a Mohs hardness of about 3.5.

In plane-polarized incident light, fettelite from Chañarcillo is grayish white in color, with moderate bireflectance (from white to brownish gray). Under crossed polars, it shows weak anisotropism with strong red internal reflections. Reflectance measurements were performed in air by means of a MPM-200 Zeiss microphotometer equipped with a MSP-20 system processor on a Zeiss Axioplan ore microscope. The filament temperature was approximately 3350 K. An interference filter was adjusted to, in turn, select four wavelengths for measurement (471.1, 548.3, 586.6, and 652.3 nm). Readings were taken for the specimen and standard (SiC) under the same focus conditions. The diameter of the circular measuring area was 0.1 mm. Reflectance percentages for R_{min} and R_{max} are 29.7, 30.4 (471.1 nm); 26.5, 28.9 (548.3 nm); 25.2, 26.7 (586.6 nm); and 22.9, 23.7 (652.3 nm), respectively. Fettelite from Chañarcillo appears to be slightly less reflective than that from the type locality (Wang and Paniagua 1996).

Solution and refinement of the structure

Data collection on the selected crystal was done with an Oxford Diffraction Xcalibur 3 diffractometer (X-ray Mo$K\alpha$ radiation, $\lambda = 0.71073$ Å) fitted with a Sapphire 2 CCD detector (see Table 2 for details). In expectation of possible crystal twinning, a full diffraction sphere was collected. The diffraction pattern was apparently consistent with trigonal symmetry ($a \approx 15.1$ Å and $c \approx 15.5$ Å). Intensity integration and standard Lorentz-polarization corrections were done with the CrysAlis RED (Oxford Diffraction 2006) software package. The program ABSPACK of the CrysAlis RED package (Oxford Diffraction 2006) was used for the absorption correction. Subsequent calculations were conducted with the JANA2000 program suite (Petříček et al. 2000).

Wang and Paniagua (1996) reported that fettelite could have crystallized in one of the following possible space groups: $P312$, $P321$, $P31m$, $P3m1$, $P\bar{3}1m$, or $P\bar{3}m1$. Following these authors, the collected data were initially merged according to point groups $\bar{3}$ ($R_{int} = 0.2543$), $\bar{3}m1$ ($R_{int} = 0.1562$), and $\bar{3}1m$ ($R_{int} = 0.2927$). Despite the high R value of merging of reflections in the $\bar{3}m1$ point

TABLE 2. Data and experimental details for the selected fettelite crystal

Crystal data	
Formula	$[Ag_6As_2S_7][Ag_{10}HgAs_2S_8]$
Crystal size (mm)	0.095 × 0.088 × 0.012
Form	platy
Color	red
Crystal system	monoclinic
Space group	*C*2
a (Å)	26.0388(10)
b (Å)	15.0651(8)
c (Å)	15.5361(8)
β (°)	90.48(1)
V (Å^3)	6094.2(5)
Z	8
Data collection	
Instrument	Oxford Diffraction Excalibur 3
Radiation type	Mo*K*α (λ = 0.71073)
Temperature (K)	298(3)
Detector to sample distance (cm)	5
Number of frames	3558
Measuring time(s)	40
Maximum covered 2θ(°)	69.52
Absorption correction	multi-scan (ABSPACK; Oxford Diffraction 2006)
Collected reflections	73858
Unique reflections	17447
Reflections with $F_o > 4\sigma(F_o)$	7143
R_{int}	0.0673
R_σ	0.0612
Range of *hkl*	$-41 \le h \le 41$, $-23 \le k \le 23$, $-24 \le l \le 24$
Refinement	
Refinement	Full-matrix least squares on F^2
Twin matrices	$\begin{bmatrix}1&0&0\\0&1&0\\0&0&1\end{bmatrix}$, $\begin{bmatrix}-0.5&-0.5&0\\1.5&-0.5&0\\0&0&1\end{bmatrix}$, $\begin{bmatrix}-0.5&0.5&0\\-1.5&-0.5&0\\0&0&1\end{bmatrix}$, $\begin{bmatrix}-1&0&0\\0&-1&0\\0&0&-1\end{bmatrix}$, $\begin{bmatrix}0.5&0.5&0\\-1.5&0.5&0\\0&0&1\end{bmatrix}$, $\begin{bmatrix}0.5&-0.5&0\\1.5&0.5&0\\0&0&1\end{bmatrix}$
Twin volume fractions	0.4111(8), 0.3925(5), 0.1177(4) 0.0302(3), 0.0275(3), 0.0210(3)
Final $R_{(obs)}$ [$I > 2\sigma(I)$]	0.0656
Final R (all data)	0.0759
Number of least squares parameters	657
$\Delta\rho_{max}$ (e Å^{-3})	1.73
$\Delta\rho_{min}$ (e Å^{-3})	−1.77

group (which could be due to an incorrect absorption correction), the structure was preliminarily solved in the $P\bar{3}m1$ space group by using the $Ag_{24}HgAs_5S_{20}$ stoichiometry reported by Wang and Paniagua (1996). A residual $R = 0.20$ value was quickly achieved. However, the preliminary structural model obtained in this study indicated a different stoichiometry (i.e., $Ag_{16}HgAs_4S_{15}$) than that previously reported (i.e., $Ag_{24}HgAs_5S_{20}$) and a large spreading of the silver electron density in the $[Ag_{10}HgAs_2S_8]^{2+}$ pseudo layer (the *B* layer, see the structure description). The structure model was subsequently optimized and an ordered model was sought, but no improvement in *R* could be achieved. It was then obvious that the symmetry was not correct and a new structure model was established, with a different crystal symmetry. The reflection data set was transformed in the *C*-centered orthohexagonal cell (with $a \approx 3^{1/2} b$; i.e., $a \approx 26$, $b \approx 15$ Å, and $c \approx 15.5$ Å) according to the transformation matrix |210/010/001| and averaged accordingly in the monoclinic symmetry ($R_{int} = 0.0673$), taking into account the twin law that makes the twin lattice hexagonal (i.e., twinning by metric merohedry; Nespolo 2004 and references therein). For details on the averaging of equivalent reflections for twins in JANA2000, see Gaudin et al. (2000). Once again, the structure refinement was initiated in space group $C2/m$. A better solution was found ($R = 0.15$), but with numerous partially occupied sites for Ag in the $[Ag_{10}HgAs_2S_8]^{2+}$ *B* layer and very large atomic displacement parameters. At this point, a thorough analysis of the structure (essentially based upon the observation of the very large atomic displacement parameters for particular atoms) suggested that the mirror symmetry element of space group $C2/m$ should be removed. The reflection and atomic position data sets were then adapted to the *C*2 space group and the structure refined. Given the large number of atoms in the starting structural model, the site-occupancy refinement of most of the metal positions, and the use of anisotropic atomic displacement parameters for all the atoms, a severe damping factor (<0.1) was used in the full-matrix refinement.

After several cycles, an ordered solution with full site occupancies was finally determined by carefully removing atoms with low site occupations and/or non-realistic distances with neighboring atoms and adding significant positions found in the difference Fourier syntheses. The structure could be smoothly refined in *C*2 without any damping factor or restrictions. The refinement of the occupancy factors for all Hg (Hg vs. Cu) and Ag (Ag vs. Cu) atoms produced site-scattering values consistent with pure metals. On the other hand, some of the As atoms were found to be partially replaced by Sb (Table 3). At this stage, the residual value converged to $R = 0.072$ for observed reflections [$I > 2\sigma(I)$], including all the collected reflections in the refinement. Based on this refinement, the analyses of the difference Fourier synthesis maps suggested an additional twin law with a twofold axis, perpendicular to the previous threefold axis as a generator twin element, thus leading to a second-degree twin. The introduction of only three new parameters (the new twin volume ratios) lowered the *R* value to 0.068, although the new domains were rather small in size [3.02(5), 2.75(3), and 2.10(5)%]. At the last stage, with anisotropic atomic displacement parameters for all atoms and no constraints, the residual value settled at $R = 0.0656$ for 7143 independent observed reflections [$I > 2\sigma(I)$] and 657 parameters and at $R = 0.0759$ for all 17 447 independent reflections.

Table 2 reports further details of the refinement. Atom coordinates and isotropic displacement parameters are given in Table 3. Table 4[1] reports the anisotropic displacement parameters and Table 5[1] lists the observed and calculated structure factors.

DESCRIPTION OF THE STRUCTURE

Although fettelite cannot be considered a layered compound, its structure can be easily described as a regular alteration of two kinds of layers along the **c**-axis (Fig. 1): a first layer (labeled *A*), ~6.50 Å thick, with general composition $[Ag_6As_2S_7]^{2-}$ and a second layer (labeled *B*), ~9.00 Å thick, with general composition $[Ag_{10}HgAs_2S_8]^{2+}$. The analysis of each module cannot be made

[1] Deposit item AM-09-015, Tables 4 and 5 (anisotropic displacement parameters and the observed and calculated structure factors, respectively) and a CIF. Deposit items are available two ways: For a paper copy contact the Business Office of the Mineralogical Society of America (see inside front cover of recent issue) for price information. For an electronic copy visit the MSA web site at http://www.minsocam.org, go to the American Mineralogist Contents, find the table of contents for the specific volume/issue wanted, and then click on the deposit link there.

independently because some atoms have coordinating atoms in the other module.

In the $[Ag_6As_2S_7]^{2-}$ *A* module layer (Fig. 2a), each silver cation is coordinated to three sulfur atoms. The mean Ag-S bond distances are in the range 2.44–2.55 Å with an overall mean of 2.50 Å. In the $[AsS_3]^{3-}$ pyramids belonging to this layer (i.e., As1, As2, As3, and As4), the overall mean As-S bond distance (2.23 Å) is consistent with the value observed in the crystal structure of proustite, $Ag_3[AsS_3]$ (2.293 Å, Engel and Nowacki 1966), and those observed for the different polytypes of pearceite (i.e., 2.31, 2.26, and 2.27 Å for the -*Tac*, -*T2ac*, and -*M2a2b2c* polytypes, respectively; Bindi et al. 2006a, 2007b).

In the $[Ag_{10}HgAs_2S_8]^{2+}$ *B* module layer (Fig. 3), the remaining 22 independent Ag atoms adopt various coordinations extending from quasi linear to quasi tetrahedral (Table 6). In detail, four silver atoms (i.e., Ag20, Ag29, Ag32, and Ag34) can be considered in linear coordination with an overall mean Ag-S of 2.46 Å, although the S-Ag-S angles always depart from 180°. One Ag atom (i.e., Ag33) may be considered as threefold coordinated with a mean Ag-S distance of 2.58 Å, in good agreement with both the Ag-S distance found for the Ag(1) position in the crystal structure of stephanite, $Ag_5[S|SbS_3]$ (2.54 Å: Ribár and Nowacki 1970) and that found for the Ag position in the crystal structure of pyrargyrite, $Ag_3[SbS_3]$ (2.573 Å: Engel and Nowacki 1966). The last 17 silver atoms (i.e., Ag13, Ag14, Ag15, Ag16, Ag17, Ag18, Ag19, Ag21, Ag22, Ag23, Ag24, Ag25, Ag26, Ag27, Ag28, Ag30, and Ag31) adopt a close-to-tetrahedral coordination with an overall mean Ag-S distance of 2.64 Å, which

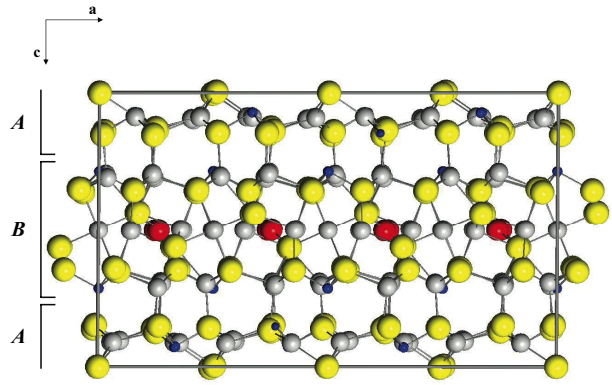

FIGURE 1. Projection of the fettelite structure along the monoclinic *b* axis, emphasizing the succession of the $[Ag_6As_2S_7]^{2-}$ *A* and $[Ag_{10}HgAs_2S_8]^{2+}$ *B* module layers. Gray, blue, red, and yellow circles indicate Ag, As, Hg, and S atoms, respectively. The unit cell is outlined. (Color online.)

TABLE 3. Site occupancy refinement (*s.o.f.*), atom coordinates and equivalent isotropic-displacement parameters (Å²) for fettelite

Atom	*s.o.f.*	*x*	*y*	*z*	U_{eq}
Hg1	1	0.12320(6)	0.10984(8)	0.50147(9)	0.0360(3)
Hg2	1	0.13062(5)	0.61547(8)	0.50052(9)	0.0360(3)
Ag1	1	0.27953(9)	0.8412(1)	0.9149(1)	0.0307(5)
Ag2	1	0.0779(1)	0.4708(1)	0.0866(2)	0.0353(6)
Ag3	1	0.04809(9)	0.6250(1)	−0.0958(1)	0.0314(5)
Ag4	1	−0.02875(9)	0.3891(1)	0.0898(1)	0.0285(5)
Ag5	1	−0.03269(9)	−0.1126(1)	0.0903(1)	0.0336(6)
Ag6	1	0.0774(1)	−0.0199(1)	0.0867(2)	0.0355(6)
Ag7	1	0.04708(9)	0.1234(1)	0.9050(1)	0.0328(5)
Ag8	1	0.1669(1)	0.2503(1)	0.9109(2)	0.0339(6)
Ag9	1	0.20505(8)	0.1017(1)	0.0980(1)	0.0290(6)
Ag10	1	0.28171(9)	0.3295(1)	0.9117(1)	0.0344(6)
Ag11	1	0.1785(1)	0.7510(1)	0.9124(2)	0.0365(6)
Ag12	1	0.20053(9)	0.6158(1)	0.0937(1)	0.0330(5)
Ag13	1	0.12915(9)	−0.1234(1)	0.7115(1)	0.0332(5)
Ag14	1	0.11721(8)	0.6314(1)	0.3025(1)	0.0315(5)
Ag15	1	0.01754(9)	0.7331(1)	0.3082(1)	0.0316(5)
Ag16	1	0.01463(9)	0.2324(1)	0.2960(1)	0.0316(5)
Ag17	1	0.13128(9)	0.3792(1)	0.7070(2)	0.0338(6)
Ag18	1	0.2356(1)	0.4881(1)	0.6979(2)	0.0345(6)
Ag19	1	0.11999(9)	0.1351(1)	0.3084(1)	0.0335(5)
Ag20	1	0	0.7553(2)	½	0.0358(9)
Ag21	1	0.13653(8)	0.0792(1)	0.6901(1)	0.0253(5)
Ag22	1	0.18308(8)	0.2989(1)	0.5006(1)	0.0275(5)
Ag23	1	0.1381(1)	0.5810(1)	0.6946(2)	0.0375(6)
Ag24	1	0.11439(9)	0.3315(1)	0.2991(1)	0.0345(5)
Ag25	1	0.17871(9)	0.8062(1)	0.4976(1)	0.0353(5)
Ag26	1	0.2345(1)	−0.0113(1)	0.6951(2)	0.0355(6)
Ag27	1	0.06948(9)	−0.0801(1)	0.5021(1)	0.0323(5)
Ag28	1	0.11638(9)	0.8386(1)	0.2938(1)	0.0288(5)
Ag29	1	0.24814(8)	0.1456(1)	0.5009(1)	0.0335(5)
Ag30	1	0	0.2931(2)	½	0.0364(8)
Ag31	1	0.24920(9)	0.4541(2)	0.5018(2)	0.0331(6)
Ag32	1	0	0.1002(2)	½	0.0378(8)
Ag33	1	0.07288(9)	0.4245(1)	0.5011(1)	0.0336(6)
Ag34	1	0	0.5604(2)	½	0.0313(9)
As1	1	0.0851(1)	0.2307(1)	0.0728(2)	0.0217(6)
As2	1	0.0806(1)	0.7307(2)	0.0738(2)	0.0253(7)
As3	0.725(2)	0.1669(1)	0.4913(1)	0.9289(2)	0.0246(9)
Sb3	0.275	0.1669	0.4913	0.9289	0.0246
As4	0.841(3)	0.1692(1)	−0.0067(1)	0.9268(2)	0.0225(9)
Sb4	0.159	0.1692	−0.0067	0.9268	0.0225
As5	1	0.2487(1)	0.7381(1)	0.2850(2)	0.0209(6)
As6	0.789(3)	0.0002(1)	0.4774(1)	0.2858(2)	0.0218(8)
Sb6	0.211	0.0002	0.4774	0.2858	0.0218
As7	0.838(2)	0.0012(1)	−0.0188(1)	0.7148(2)	0.0223(9)
Sb7	0.162	0.0012	−0.0188	0.7148	0.0223
As8	1	0.2506(1)	0.2385(2)	0.2848(2)	0.0250(7)
S1	1	0.0064(3)	0.7478(4)	0.1519(5)	0.028(2)
S2	1	0.1173(2)	0.1155(4)	0.1525(4)	0.024(1)
S3	1	0.2429(3)	0.4715(4)	0.8579(4)	0.025(2)
S4	1	0.1350(2)	0.6087(3)	0.8548(4)	0.018(1)
S5	1	0.0105(3)	0.2481(3)	0.1396(4)	0.023(2)
S6	1	0.1258(3)	−0.1116(3)	0.8735(4)	0.023(1)
S7	1	0.1204(3)	0.3828(4)	0.8622(4)	0.024(1)
S8	1	0.1227(3)	0.8454(3)	0.1289(4)	0.022(1)
S9	1	0.1128(3)	0.6157(4)	0.1467(4)	0.028(2)
S10	1	0.1259(3)	0.3399(4)	0.1334(4)	0.027(2)
S11	1	0.2412(3)	−0.0222(4)	0.8569(5)	0.025(2)
S12	1	0.2541(2)	0.7060(4)	−0.0035(4)	0.026(2)
S13	1	0.1316(3)	0.1011(3)	0.8502(4)	0.023(1)
S14	1	0	0.5194(5)	0	0.026(2)
S15	1	0	0.0196(5)	0	0.023(2)
S16	1	0.2131(3)	0.8538(4)	0.3592(4)	0.023(2)
S17	1	0.0753(3)	−0.0205(3)	0.3542(4)	0.025(2)
S18	1	0.0858(3)	0.7411(3)	0.4348(4)	0.020(1)
S19	1	0.0829(3)	0.2334(3)	0.4367(4)	0.018(1)
S20	1	0.1663(3)	−0.0215(3)	0.5604(4)	0.022(2)
S21	1	0.2127(2)	0.6207(4)	0.3506(4)	0.019(1)
S22	1	0.0740(3)	0.4778(4)	0.3518(4)	0.024(2)
S23	1	0.0439(3)	−0.1278(4)	0.6517(4)	0.027(2)
S24	1	−0.0379(3)	0.3667(3)	0.3497(4)	0.022(1)
S25	1	−0.0366(3)	0.5928(3)	0.3545(4)	0.025(2)
S26	1	0.1744(3)	0.2443(3)	0.6456(4)	0.022(1)
S27	1	0.2113(3)	0.3538(4)	0.3564(4)	0.024(2)
S28	1	0.2859(2)	0.6229(4)	0.6494(4)	0.020(1)
S29	1	−0.0341(3)	0.0945(3)	0.3608(4)	0.029(2)
S30	1	0.1696(2)	0.7348(3)	0.6456(4)	0.018(1)
S31	1	0.1612(3)	0.4833(3)	0.5619(4)	0.023(2)

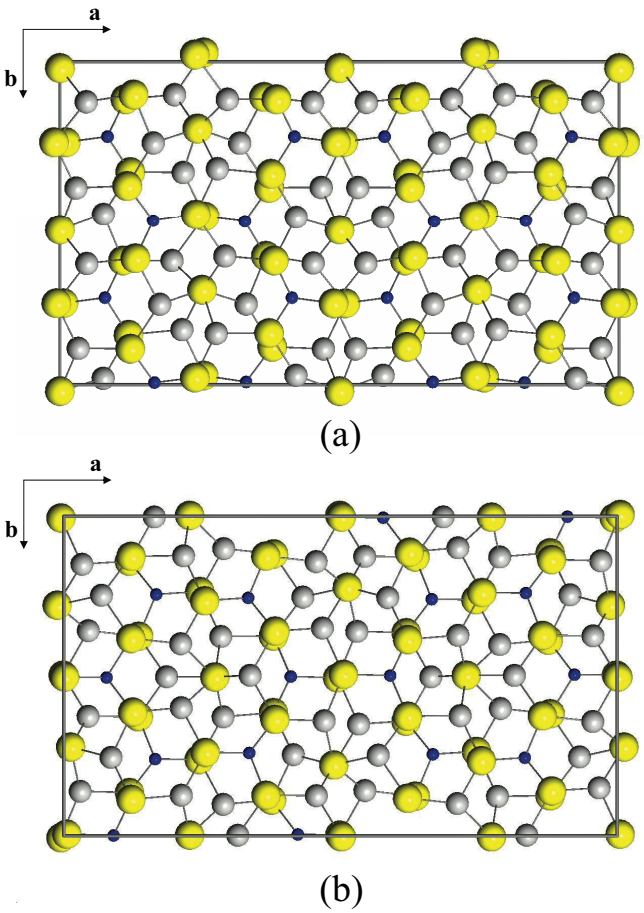

FIGURE 2. [001] projection of the *A* module layer of fettelite (**a**) and pearceite-*M*2*a*2*b*2*c* (Bindi et al. 2007b) (**b**). Gray, blue, and yellow circles indicate Ag, As, and S atoms, respectively. The superposition of the two layers is obtained by translating the origin of the layer of fettelite by ¼ **b**. (Color online.)

matches that found for the Ag3 position in the crystal structure of stephanite, $Ag_5[S|SbS_3]$ (2.68 Å: Ribár and Nowacki 1970). In the $[AsS_3]^{3-}$ pyramids belonging to this layer (i.e., As5, As6, As7, and As8), the overall mean As-S bond distance (2.25 Å) is again consistent with the value observed in the crystal structure of proustite and those observed for the different polytypes of pearceite. Finally, the two mercury atoms exhibit a nearly perfect linear coordination, with similar mean Hg-S distances (overall mean Hg-S = 2.395 Å). These distances are in good agreement with those found in $\{Hg[S(CH_2)_2NH_3]_2\}(C1)_2$, where Hg shows a similar linear coordination with sulfur (Hg-S: 2.333 and 2.338 Å; Kim et al. 2002). It is worth noting that the shortest Ag-Ag contact observed (Ag30-Ag33 = 2.75 Å) is slightly shorter than that found in pure silver (i.e., 2.89 Å).

On the basis of information gained from this characterization, the crystal chemical formula originally reported by Wang and Paniagua (1996) was revised according to the structural results, yielding $[Ag_6As_2S_7][Ag_{10}HgAs_2S_8]$ ($Z = 8$). The refined composition, $[Ag_6(As_{1.78}Sb_{0.22})_{\Sigma=2}S_7][Ag_{10}Hg(As_{1.82}Sb_{0.18})_{\Sigma=2}S_8]$, is in excellent agreement with that obtained by the electron microprobe analysis.

Table 7 compares the X-ray powder pattern originally reported by Wang and Paniagua (1996) with that calculated using the structural parameters obtained in this study. Calculated and observed data are in good agreement.

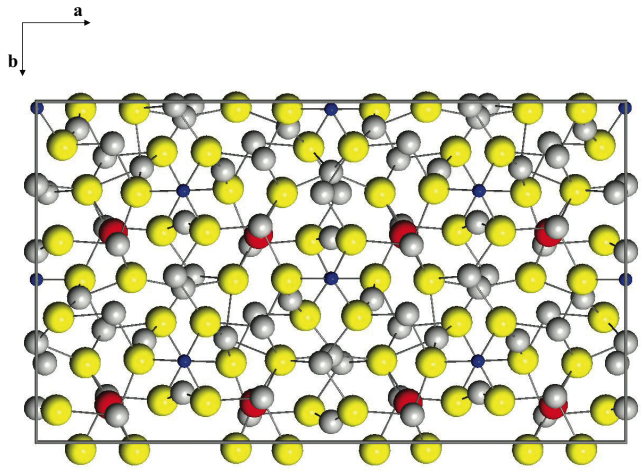

FIGURE 3. [001] projection of the *B* module layer of fettelite. Gray, blue, red, and yellow circles indicate Ag, As, Hg, and S atoms, respectively. (Color online.)

RELATIONSHIPS WITH THE PEARCEITE-POLYBASITE GROUP OF MINERALS

Fettelite shows a strong similarity with minerals belonging to the pearceite-polybasite group (Bindi et al. 2007a). The solution of the crystal structure shows that fettelite possesses a module layer with composition $[Ag_6As_2S_7]^{2-}$ (i.e., the *A* layer; Fig. 2a) identical to that observed in the pearceite-polybasite minerals (Fig. 2b). On the other hand, the *B* module layer is different, mainly due to the presence of Hg, two additional As atoms and more silver atoms. As documented by Bindi et al. (2006b), the pearceite-polybasite minerals show three different unit-cell types: 111 (polytype -*Tac*), 221 (polytype -*T*2*ac*), and 222 (polytype -*M*2*a*2*b*2*c*), which represent the strongly disordered (space group $P\bar{3}m1$), partially ordered (space group *P*321), and fully ordered form (space group *C*2/*c*), respectively. In this light, fettelite could represent the fully ordered form stable at room temperature. It could convert to a disordered form at high temperature, where the disorder could give rise to a folding of the cell along the *a* and *b* directions, as found in the 111 structures of the pearceite-polybasite minerals (Bindi et al. 2006b). However, this mechanism needs to be confirmed through the elucidation of the fettelite structure at high temperature, which is currently in progress.

RELATIONSHIPS WITH THE TYPE FETTELITE

If we compare the unit-cell parameters obtained for the fettelite from Chañarcillo [$a = 26.0388(10)$, $b = 15.0651(8)$, $c = 15.5361(8)$ Å, $\beta = 90.48(1)°$, and $V = 6094.2(5)$ Å^3] with those reported by Wang and Paniagua (1996) for the type fettelite (transformed in monoclinic setting: $a = 25.98$, $b = 15.00$, $c = 15.46$ Å, $\beta = 90.00°$, and $V = 6024$ Å^3), we observe that the mineral studied here exhibits a unit-cell volume greater than that observed for the mineral from the type locality. The increase in the unit-cell volume is isotropic with respect to the unit-cell

TABLE 6. Main interatomic distances (Å) and their standard deviations (in parentheses) for the selected fettelite crystal

$[Ag_6(As,Sb)_2S_7]^{2-}$ *A* layer					
As1-S10	2.169(7)	As2-S8	2.215(6)		
As1-S5	2.226(7)	As2-S9	2.271(6)		
As1-S2	2.287(6)	As2-S1	2.305(7)		
<As1-S>	2.227	<As2-S>	2.250		
As3-S4	2.264(7)	As4-S6	2.108(7)		
As3-S7	2.278(6)	As4-S11	2.187(7)		
As3-S3	2.293(7)	As4-S13	2.234(7)		
<As1-S>	2.279	<As1-S>	2.177		
Ag1-S11	2.455(7)	Ag2-S10	2.442(7)	Ag3-S4	2.408(6)
Ag1-S12	2.492(6)	Ag2-S14	2.533(4)	Ag3-S1	2.485(7)
Ag1-S10	2.580(6)	Ag2-S9	2.539(7)	Ag3-S14	2.519(5)
<Ag1-S>	2.509	<Ag2-S>	2.505	<Ag3-S>	2.471
Ag4-S5	2.478(6)	Ag5-S6	2.494(7)	Ag6-S8	2.434(6)
Ag4-S7	2.508(6)	Ag5-S1	2.522(7)	Ag6-S15	2.487(4)
Ag4-S14	2.525(6)	Ag5-S15	2.584(6)	Ag6-S2	2.504(7)
<Ag4-S>	2.504	<Ag5-S>	2.533	<Ag6-S>	2.475
Ag7-S13	2.390(6)	Ag8-S7	2.451(6)	Ag9-S12	2.405(6)
Ag7-S15	2.481(5)	Ag8-S12	2.588(7)	Ag9-S2	2.452(6)
Ag7-S5	2.498(7)	Ag8-S13	2.602(6)	Ag9-S3	2.478(7)
<Ag7-S>	2.457	<Ag8-S>	2.547	<Ag9-S>	2.445
Ag10-S3	2.506(7)	Ag11-S12	2.449(7)	Ag12-S9	2.435(6)
Ag10-S12	2.527(6)	Ag11-S6	2.553(6)	Ag12-S12	2.471(6)
Ag10-S8	2.584(6)	Ag11-S4	2.581(6)	Ag12-S11	2.682(7)
<Ag10-S>	2.539	<Ag11-S>	2.528	<Ag12-S>	2.529
$[Ag_{10}Hg(As,Sb)_2S_8]^{2+}$ *B* layer					
As5-S21	2.250(7)	As6-S22	2.171(7)		
As5-S26	2.268(7)	As6-S24	2.184(6)		
As5-S16	2.290(6)	As6-S25	2.258(7)		
<As5-S>	2.269	<As6-S>	2.204		
As7-S23	2.216(6)	As8-S28	2.236(7)		
As7-S29	2.246(6)	As8-S27	2.307(7)		
As7-S17	2.254(7)	As8-S30	2.335(7)		
<As7-S>	2.239	<As8-S>	2.292		
Hg1-S19	2.358(6)	Hg2-S31	2.344(6)		
Hg1-S20	2.449(6)	Hg2-S18	2.443(6)		
<Hg1-S>	2.403	<Hg2-S>	2.393		
Ag20-S18	2.470(6)	Ag29-S28	2.514(7)	Ag32-S29	2.333(8)
Ag20-S18	2.470(6)	Ag29-S21	2.542(7)	Ag32-S29	2.333(8)
<Ag20-S>	2.470	<Ag29-S>	2.528	<Ag32-S>	2.333
Ag34-S25	2.494(7)	Ag33-S22	2.455(7)	Ag13-S23	2.400(8)
Ag34-S25	2.494(7)	Ag33-S31	2.632(8)	Ag13-S6	2.525(7)
<Ag34-S>	2.494	Ag33-S24	2.645(6)	Ag13-S30	2.596(5)
		<Ag33-S>	2.578	Ag13-S20	2.973(6)
				<Ag13-S>	2.624
Ag14-S9	2.434(7)	Ag15-S1	2.453(8)	Ag16-S5	2.443(6)
Ag14-S21	2.595(7)	Ag15-S18	2.643(8)	Ag16-S24	2.585(6)
Ag14-S22	2.687(6)	Ag15-S25	2.644(6)	Ag16-S29	2.638(6)
Ag14-S18	2.766(6)	Ag15-S23	2.712(6)	Ag16-S19	2.806(7)
<Ag14-S>	2.621	<Ag15-S>	2.613	<Ag16-S>	2.618
Ag17-S7	2.431(7)	Ag18-S3	2.504(7)	Ag19-S2	2.440(7)
Ag17-S26	2.514(6)	Ag18-S28	2.535(6)	Ag19-S28	2.538(7)
Ag17-S24	2.586(8)	Ag18-S16	2.586(6)	Ag19-S19	2.670(5)
Ag17-S31	2.860(6)	Ag18-S31	2.856(8)	Ag19-S17	2.715(6)
<Ag17-S>	2.598	<Ag18-S>	2.620	<Ag19-S>	2.591
Ag21-S13	2.514(6)	Ag22-S26	2.411(6)	Ag23-S4	2.526(6)
Ag21-S20	2.644(6)	Ag22-S27	2.504(6)	Ag23-S30	2.575(5)
Ag21-S26	2.766(5)	Ag22-S19	2.953(7)	Ag23-S31	2.608(6)
Ag21-S29	2.785(8)	Ag22-S31	2.993(7)	Ag23-S25	2.750(8)
<Ag21-S>	2.677	<Ag22-S>	2.715	<Ag23-S>	2.615
Ag24-S22	2.579(6)	Ag25-S16	2.444(6)	Ag26-S21	2.523(6)
Ag24-S10	2.597(6)	Ag25-S30	2.551(6)	Ag26-S11	2.524(7)
Ag24-S27	2.690(8)	Ag25-S18	2.780(8)	Ag26-S27	2.604(6)
Ag24-S19	2.731(5)	Ag25-S20	2.793(6)	Ag26-S20	2.738(8)
<Ag24-S>	2.649	<Ag25-S>	2.642	<Ag26-S>	2.597
Ag27-S17	2.473(7)	Ag28-S17	2.559(6)	Ag30-S19	2.544(6)
Ag27-S23	2.527(6)	Ag28-S8	2.571(6)	Ag30-S19	2.544(6)
Ag27-S20	2.814(7)	Ag28-S16	2.718(8)	Ag30-S24	2.760(7)
Ag27-S18	2.922(5)	Ag28-S18	2.760(6)	Ag30-S24	2.760(7)
<Ag27-S>	2.684	<Ag28-S>	2.652	<Ag30-S>	2.652
Ag31-S20	2.438(6)				
Ag31-S31	2.520(6)				
Ag31-S16	2.806(7)				
Ag31-S27	2.885(7)				
<Ag31-S>	2.662				

TABLE 7. X–ray powder diffraction patterns for fettelite

	1			2	
hkl	d_{calc} (Å)	I/I_o	*hkl*	d_{obs} (Å)	I/I_o
001	15.5356	31.92	–	–	–
002	7.7678	19.95	002	7.69	1
021	6.7779	3.14	–	–	–
$\bar{4}01$	6.0218	6.34	–	–	–
221	6.0029	9.34	201	5.97	1
$\bar{2}22$	5.0043	7.55	022	4.98	1
$\bar{4}22$	4.1715	4.29		–	
620	3.7602	3.42		–	
440	3.2599	19.72	400	3.243	2
800	3.2547	9.76			
$\bar{8}01$	3.1909	25.86	401	3.175	6
441	3.1878	44.78			
005	3.1071	100.00	005	3.091	10
043	3.0459	3.39			
$\bar{8}02$	3.0109	17.28	402	2.998	4
442	3.0015	35.84			
$\bar{8}21$	2.9382	10.87	321	2.925	1
821	2.9298	10.48			
640	2.8444	6.21	–	–	–
$\bar{8}22$	2.7958	5.62	–	–	–
641	2.7952	3.79	–	–	–
822	2.7814	3.51	–	–	–
$\bar{8}03$	2.7661	5.18	–	–	–
$\bar{4}43$	2.7641	26.68	043	2.755	3
443	2.7536	10.90			
803	2.7453	12.80			
$\bar{6}42$	2.6757	7.36	412	2.667	1
823	2.5793	3.53	–	–	–
060	2.5108	4.52	–	–	–
$\bar{4}44$	2.5021	31.69	330,044	2.497	2
643	2.4873	5.25			
804	2.4844	17.21	331	2.471	2
260	2.4654	3.95	–	–	–
$\bar{2}61$	2.4355	7.18	421	2.426	1
$\bar{8}41$	2.4346	5.96			
10 21	2.4276	6.55	–	–	–
062	2.3891	4.96	–	–	–
$\bar{8}24$	2.3770	5.64	–	–	–
063	2.2593	6.03	–	–	–
$\bar{8}05$	2.2569	4.62	–	–	–
$\bar{4}45$	2.2539	3.85	333,405	2.245	1
445	2.2445	9.57			
$\bar{10}$ 42	2.0684	4.20	424	2.076	2
$\bar{8}06$	2.0346	4.20	–	–	–
$\bar{4}46$	2.0317	6.46	–	–	–
446	2.0234	7.22	–	–	–
806	2.0181	3.56	–	–	–
663	2.0010	3.22	–	–	–
$\bar{8}26$	1.9642	5.23	–	–	–
065	1.9529	3.94	–	–	–
826	1.9493	3.99	–	–	–
845	1.9240	3.01	–	–	–
080	1.8831	9.37	440	1.878	8
12 40	1.8801	28.21			
$\bar{8}07$	1.8408	6.56	–	–	–
447	1.8310	12.36	407,442	1.825	1
$\bar{4}48$	1.6714	3.23	540,408	1.664	1
$\bar{8}81$	1.6218	4.37	–	–	–
$\bar{12}$ 45	1.6138	8.27	081	1.613	2
085	1.6104	4.77	–	–	–
12 45	1.6034	7.57	–	–	–
00 10	1.5536	5.24	319	1.553	1
$\bar{4}49$	1.5282	5.05			
$\bar{16}$ 04	1.5054	3.17	–	–	–
884	1.5007	3.80	–	–	–

Notes: 1 = calculated powder pattern and indexing for fettelite of this study. *d* values calculated on the basis of a = 26.0388(10) Å, b = 15.0651(8) Å, c = 15.5361(8) Å, and β = 90.48(1)°, and with the atomic coordinates reported in Table 3. Intensities calculated using XPOW software version 2.0 (Downs et al. 1993). 2 = observed powder pattern and indexing originally reported by Wang and Paniagua (1996).

parameters. A reason for the observed larger unit-cell volume for the mineral studied here could be linked to a different Ag/Hg ratio. Indeed, if we recalculate the chemical formula of fettelite from the type locality (Wang and Paniagua 1996) based on 36 atoms, we obtain $Ag_{17.19}Cu_{0.03}Pb_{0.01}Fe_{0.02}Tl_{0.02}Hg_{0.71}As_{3.59}Sb_{0.05}S_{14.38}$ (Table 1). This means that the Hg positions in the type fettelite could be filled by Ag and/or Cu, thus decreasing the unit-cell volume. Nevertheless, an excess of 0.90 silver apfu remains. This inconsistency could be linked to non-optimal EMPA conditions used by Wang and Paniagua (1996). However, reflectivity measurements show that fettelite from Chañarcillo is slightly less reflective than that from the type locality, which is consistent with its lower Ag/Hg ratio, and thus corroborate the hypothesis that Ag replaces Hg in type fettelite.

Is the mineral sanguinite the same as fettelite?

Miers (1890) described a mineral from Chañarcillo, which he named sanguinite that appears to be identical to fettelite. It occurs as "fine glittering scales" on specimens of argentite "octahedra implanted on quartz or calcite, and associated with proustite and little asbestos" (palygorskite?). The description of the physical properties of sanguinite agrees well with those of the specimen used for this study. Chemical tests on ~50 scales weighing <0.0003 g showed the presence of Ag, As, and S. Miers had no reason to suspect and test for the presence of mercury. Lacking a chemical formula, sanguinite was never accorded species status. The Harvard collection has a specimen (82530), acquired in 1912, from Chañarcillo labeled sanguinite, which is composed of abundant fettelite (verified by EDS), proustite, calcite, and arsenian pyrite.

Acknowledgments

The paper benefited by the official reviews made by P. Spry and I. Pekov. Associate Editor M. Kunz is thanked for his efficient handling of the manuscript. This work was funded by M.I.U.R., P.R.I.N. 2007, project "Complexity in minerals: modulation, phase transition, structural disorder."

References cited

Bindi, L., Evain, M., and Menchetti, S. (2006a) Temperature dependence of the silver distribution in the crystal structure of natural pearceite, $(Ag,Cu)_{16}(As,Sb)_2S_{11}$. Acta Crystallographica, B62, 212–219.

Bindi, L., Evain, M., Pradel, A., Albert, S., Ribes, M., and Menchetti, S. (2006b) Fast ionic conduction character and ionic phase-transitions in disordered crystals: The complex case of the minerals of the pearceite-polybasite group. Physics and Chemistry of Minerals, 33, 677–690.

Bindi, L., Evain, M., Spry, P.G., and Menchetti, S. (2007a) The pearceite-polybasite group of minerals: Crystal chemistry and new nomenclature rules. American Mineralogist, 92, 918–925.

Bindi, L., Evain, M., and Menchetti, S. (2007b) Complex twinning, polytypism, and disorder phenomena in the crystal structures of antimonpearceite and arsenpolybasite. Canadian Mineralogist, 45, 321–333.

Cook, R.B. (1979) Famous mineral localities: Chañarcillo, Chile. Mineralogical Record, 10, 197–204.

Downs, R.T., Bartelmehs, K.L., Gibbs, G.V., and Boisen Jr., M.B. (1993) Interactive software for calculating and displaying X-ray or neutron powder diffractometer patterns of crystalline materials. American Mineralogist, 78, 1104–1107.

Engel, P. and Nowacki, W. (1966) Die verfeinerung der kristallstruktur von proustit, Ag_3AsS_3, und pyrargyrit, Ag_3SbS_3. Neues Jahrbuch für Mineralogie Monatshefte, 181–195.

Gaudin, E., Petříček, V., Boucher, F., Taulelle, F., and Evain, M. (2000) Structures and phase transitions of the A_7PSe_6 (A = Ag, Cu) argyrodite-type ionic conductors. III. α-Cu_7PSe_6. Acta Crystallographica, B56, 972–979

Kim, C-H., Parkin, S., Bharara, M., and Atwood, D. (2002) Linear coordination of Hg(II) by cysteamine. Polyhedron, 21, 225–228

Miers, H.A. (1890) Sanguinite, a new mineral, and krennerite. Mineralogical Magazine, 9, 182–184.

Nespolo, M. (2004) Twin point groups and the polychromatic symmetry of twins. Zeitschrift für Kristallographie, 219, 57–71.

Oxford Diffraction (2006) CrysAlis RED (Version 1.171.31.2) and ABSPACK in CrysAlis RED. Oxford Diffraction, Ltd., Abingdon, Oxfordshire, England.

Pérez-Priede, M., Xolans Huguet, X., Moreiras Blanco, D., and García Granda, S. (2005) Going inside fettelite, a Hg-sulfosalt mineral. Acta Crystallographica, A61, C380.

Petříček, V., Dušek, M., and Palatinus, L. (2000) JANA2000, a crystallographic computing system. Institute of Physics, Academy of Sciences of the Czech Republic, Prague.

Ribár, B. and Nowacki, W. (1970) Die Kristallstruktur von Stephanit, $[SbS_3|S|Ag_5^{III}]$. Acta Crystallographica, B26, 201–207.

Wang, N. and Paniagua, A. (1996) Fettelite, a new Hg-sulfosalt mineral from Odenwald. Neues Jahrbuch für Mineralogie Monatshefte, 313–320.

Manuscript received September 23, 2008
Manuscript accepted November 20, 2008
Manuscript handled by Martin Kunz